Paclitaxel Encapsulated in Cationic Liposomes Increases Tumor Microvessel Leakiness and Improves Therapeutic Efficacy in Combination with Cisplatin

Sebastian Strieth,[1,2] Martin E. Eichhorn,[3] Alexander Werner,[4] Birgitta Sauer,[5] Michael Teifel,[6] Uwe Michaelis,[5] Alexander Berghaus,[2] and Marc Dellian[1,2]

Abstract

Purpose: Paclitaxel encapsulated in cationic liposomes (EndoTAG-1) is a vascular targeting formulation for the treatment of solid tumors. It triggers intratumoral microthrombosis, causing significant inhibition of tumor perfusion and tumor growth associated with endothelial cell apoptosis. Here, we quantified the effects of repeated EndoTAG-1 therapy on tumor microvascular leakiness with respect to leukocyte-endothelial cell interactions, the targeting property of cationic liposomes, and the therapeutic combination with conventional cisplatin chemotherapy.

Experimental Design: Using dorsal skinfold chamber preparations in Syrian Golden hamsters, *in vivo* fluorescence microscopy experiments were done after repeated EndoTAG-1 treatment of A-Mel-3 tumors. Controls received glucose, paclitaxel alone, or cationic liposomes devoid of paclitaxel. Extravasation of rhodamine-labeled albumin was measured to calculate microvessel permeability, and intratumoral leukocyte-endothelial cell interactions were quantified. Subcutaneous tumor growth was evaluated after combination therapy followed by histologic analysis.

Results: Microvascular permeability was significantly increased only after treatment with EndoTAG-1, whereas intratumoral leukocyte-endothelial cell interactions were not affected by any treatment. In separate skinfold chamber experiments, fluorescently labeled cationic liposomes kept their targeting property for tumor endothelial cells after repeated EndoTAG-1 treatment and no signs of extravasation were observed. Subcutaneous A-Mel-3 tumor growth was significantly inhibited by the combination of cisplatin and EndoTAG-1.

Conclusions: These data show that vascular targeting with EndoTAG-1 increases tumor microvessel leakiness probably due to vascular damage. This mechanism is not mediated by inflammatory leukocyte-endothelial cell interactions. Manipulating the blood-tumor barrier by repeated tumor microvessel targeting using EndoTAG-1 can effectively be combined with tumor cell–directed conventional cisplatin chemotherapy.

Tumor blood vessels are structurally abnormal, exhibiting endothelial cell gaps (~200 nm-2 μm; ref. 1), irregular pericytes (2), and basement membranes (for review, see ref. 3). Tumor cells have often direct contact to the vascular lumen, thereby contributing to the formation of the so-called mosaic blood vessels (4). Thus, leakiness is a common feature of tumor microvessels that influences the access of therapeutic substances to tumor cells. Although the barrier function of the tumor microvessel wall is defective, extravasation of fluid and macromolecules is limited due to high interstitial fluid pressure within the tumor (3).

Despite major advances in the field of antivascular therapy, little attention has been directed at tumor microvessel permeability and how it may be affected during treatment. For upcoming therapy strategies combining antivascular therapy with conventional chemotherapy, it may be crucial to know how the permeability of microvessels is manipulated and what consequences follow for the delivery of the respective therapeutic substances.

According to Denekamp (5), vascular targeting is an antivascular therapy distinct from the classic form of antiangiogenesis. The latter relies on the inhibition of the formation of new blood vessels. In contrast, vascular targeting is based on the destruction of the already existing tumor microvasculature. As in tumors hundreds of tumor cells depend on nutrition and O_2 supply by one individual microvessel, vascular targeting promises a high efficacy of therapy (6). Liposomes are widely known as potent drug delivery systems. Especially cationic liposomes have been found to selectively target angiogenic endothelial cells in tumors and appear as promising

Authors' Affiliations: [1]Institute for Surgical Research, [2]Department of Otorhinolaryngology, [3]Department of Surgery, Campus Grosshadern, University of Munich, Munich, Germany; [4]BSL BIOSERVICE Scientific Laboratories GmbH and [5]MediGene AG, Planegg, Germany; and [6]Æterna Zentaris GmbH, Frankfurt/Main, Germany

Received 10/26/07; revised 3/7/08; accepted 3/25/08.

Grant support: Munich Biotech AG, Neuried, Germany. S. Strieth was supported by grants of the Novartis Foundation for Therapeutic Research, Nürnberg, Germany. The costs of publication of this article were defrayed in part by the payment of page charges. This article must therefore be hereby marked *advertisement* in accordance with 18 U.S.C. Section 1734 solely to indicate this fact.

Requests for reprints: Sebastian Strieth, Department of Otorhinolaryngology, University of Munich, Marchioninistr. 15, 81377 Munich, Germany. Phone: 49-89-7095-0; Fax: 49-89-2180-76532; E-mail: sebastian.strieth@med.uni-muenchen.de.

doi:10.1158/1078-0432.CCR-07-4738

carriers for therapeutic substances to realize the concept of vascular targeting as shown in an earlier study (7). It was also shown earlier that selective uptake of cationic liposomes in tumor endothelial cells is not affected by the encapsulation of the cytotoxic drug paclitaxel (8). Paclitaxel encapsulated in cationic liposomes (EndoTAG-1) resulted indeed in a mechanistic switch from tumor cell toxicity toward antivascular effects *in vivo* (9). EndoTAG-1 has been shown to induce endothelial cell apoptosis and severe impairment of functional tumor microvasculature (9) by triggering intravascular thrombosis within treated tumors (10). Moreover, treatment with EndoTAG-1 significantly retarded tumor growth and delayed the incidence of metastatic disease in subcutaneously growing experimental tumors (8). With respect to these promising results, EndoTAG-1 has entered clinical phase II treating different tumor entities. However, it remains unclear how EndoTAG-1 therapy affects leakiness of tumor microvessels.

Cationic liposomes are known to interact with WBC (11). Leukocytes can be key regulators of microvessel leakiness in inflammatory reactions (12). Again, it was not clear whether leukocytes are involved in the therapeutic effects of EndoTAG-1, as hypothesized for comparable vascular targeting agents (13). Activated rolling or adhering leukocytes are able to extravasate from the tumor vessels and this inflammatory response could possibly result in changes in microvessel leakiness or in blood flow disturbances and indirect tumor cell death. Furthermore, permeability changes and vascular damage due to EndoTAG-1 could affect the targeting property of cationic liposomes especially after repeated treatment. Due to a functional tumor microvessel cutoff size of some hundred nanometers, cationic liposomes might extravasate if changes in interstitial hydrostatic pressure within tumors alter the convective movement of large solutes (3). On the other hand, diffusion of small solutes may also be affected by changes in tumor microvessel permeability. Conventional therapy often relies on small molecular substances, e.g., cisplatin. Consequently, changes in intratumoral microvessel permeability might influence the effects of a combination therapy of EndoTAG-1 with cisplatin.

It was the aim of this study to measure the effects of repeated treatment with EndoTAG-1 on microvascular permeability and leukocyte-endothelial cell interactions. In addition, we evaluated whether the endothelium in tumor blood vessels is maintained as a target for cationic liposomes even after repeated EndoTAG-1 treatment. Finally, we quantified the effects of a combination therapy of EndoTAG-1 with conventional chemotherapy using cisplatin.

Materials and Methods

Preparation and analysis of liposomes. 1,2-Dioleoyl-3-trimethylammonium-propane (DOTAP) and 1,2 dioleoyl-*sn*-glycero-3-phosphocholine (DOPC; Avanti Polar Lipids, Inc.) were used for synthesis of the liposomes. Pure paclitaxel (Synopharm) was used for encapsulation into cationic liposomes, whereas the conventional paclitaxel formulation (Taxol, Bristol-Myers-Squibb) was diluted in 5% glucose (B. Braun).

Cationic liposomes with a total lipid content of 20 mmol/L were prepared by the lipid film method followed by several cycles of extrusion. For paclitaxel containing liposomes (EndoTAG-1), 0.1 mmol DOTAP, 0.094 mmol DOPC, and 0.006 mmol paclitaxel were dissolved in 15 mL chloroform (Merck). For control experiments, cationic liposomes without paclitaxel (CL) were prepared by dissolving 0.1 mmol DOTAP and 0.1 mmol DOPC in 15 mL chloroform. For fluorescence microscopy experiments, 0.05 mmol DOTAP, 0.046 mmol DOPC, and 0.004 mmol Rh-DOPE were dissolved in 15 mL chloroform.

The particle size of the liposomes was analyzed by photon correlation spectroscopy using a Malvern Zetasizer 3000 (Malvern Instruments). Typically, suspensions exhibited a $Z_{average}$ of 180 to 200 nm.

Lipid and paclitaxel concentrations were determined by high-performance liquid chromatography using an UV/VIS detector (205 nm for lipids and 227 nm for paclitaxel). The separation and quantitation of the components was carried out using a C8 LiChrospher 60 RP-select B column (250 × 4 mm, 5 μm particle size) with a C18 precolumn. Aliquots of the samples were diluted 1:3 with tetrahydrofuran (J.T. Baker) before measurement. The procedure has been described in detail before (8–10, 14).

Dorsal skinfold chamber preparation. Experiments were done with male Syrian golden hamsters (6-8 weeks old, 55-65 g body weight). The animals were housed in single cages and had free access to tap water and standard laboratory food (ssniff, Spezialdiaeten GmbH) throughout the experiments in accordance to institutional and governmental guidelines.

To permit quantitative fluorescence analysis of tumor microcirculation *in vivo*, a dorsal skinfold chamber preparation consisting of two symmetrical titanium frames was surgically implanted into the dorsal skin as described earlier in detail (15, 16). The chambers were well tolerated and the animals showed no signs of discomfort. Following a recovery period of at least 24 h from anesthesia and microsurgery, chamber preparations fulfilling the criteria of microscopically intact microcirculation and no signs of inflammation were inoculated with 2 μL of dense tumor cell suspension (~2 × 10^5 cells) of the A-Mel-3 amelanotic melanoma of the hamster onto the striated skin muscle layer using 1 mL syringes (Becton Dickinson) and a variable (0.5-10 μL) pipette system (Eppendorf).

All surgical procedures were done under anesthesia with ketamine (100 mg/kg body weight i.p., Ketavet; Parke-Davis) and xylazine (10 mg/kg body weight i.p., Rompun; Bayer).

In vivo *fluorescence microscopy.* Permanently indwelling fine polyethylene catheters (PE10, inner diameter 0.28 mm) were implanted into the right jugular vein on day 3 after tumor cell implantation under general anesthesia, as described above. For intravital microscopy, the awake chamber bearing hamster was immobilized in a Perspex tube on a specially designed stage (Effenberger) under a modified Zeiss microscope (Axiotech Vario; Zeiss). FITC-labeled dextran (MW 500,000; 0.05-0.1 mL of a 5% solution in 0.9% NaCl; Sigma) was injected i.v. as a plasma marker to visualize tumor microcirculation. Selective observation of FITC-labeled plasma, rhodamine-labeled albumin (and leukocytes, respectively, see below) was possible using epi-illumination with a 100-W mercury lamp with selective filter blocks (Zeiss). *In vivo* fluorescence microscopic images were acquired by a SIT video camera (C2400-08; Hamamatsu) and recorded on S-VHS videotape for subsequent off-line digital analysis (Cap Image; Zeintl).

Assessment of microvascular permeability for albumin. Effective microvascular permeability for albumin was measured in a central tumor region of interest (ROI) according to the method published by Yuan et al. (17) on day 10 after tumor cell implantation.

In brief, the fluorescently labeled albumin (Molecular Probes) was dissolved in PBS and given as a bolus (10 μg/g body weight). Fluorescence intensity of tumor tissue was monitored using a ×20 objective of a fluorescence microscope and quantified over a period of 15 min. For every respective region of interest (ROI), the vascular volume/vascular surface ratio was analyzed. Tumor microvascular permeability P from experiments with six to seven individual tumors for each of the different treatment groups was calculated from these data according to the formula of Yuan et al. (17):

$$P = (1 - H_{\text{micro}})\frac{V}{S}\left(\frac{1}{I_0 - I_b}\frac{\mathrm{d}I}{\mathrm{d}t} + \frac{1}{k}\right)$$

where P is the effective microvascular permeability, H_{micro} is the microhematocrit in A-Mel-3 tumor microvessels, V is the vascular volume, S is the vascular surface in the measured intravital microscopic ROI, I_0 is the fluorescence intensity at maximal intravascular distribution of the contrast agent, I_b is the background intensity, and k is the time constant of albumin plasma clearance.

Digital image analysis (Cap Image; Zeintl), as described in detail by Zeintl and Klysz (18, 19), allows measurement of individual vessel length l and diameter d for the calculation of the ratio of vascular volume V and vascular surface S.

Evaluation of leukocyte-endothelial cell interactions. Rhodamine 6G (Molecular Probes; 0.04 mL of a 0.05% solution in 0.9% NaCl) was injected i.v. to label WBC *in vivo*. Evaluation of leukocyte-endothelial cell interactions was done on day 7 after tumor cell implantation (and thus after three treatments) in 6 ROIs in the tumor periphery and 6 ROIs in the tumor center, respectively.

Leukocyte flux was determined by counting intravascular leukocytes crossing a predefined line for 30 s. Rolling leukocytes were defined as the fraction of these cells temporarily interacting with the vessel wall and thus having a velocity at least 50% below RBC velocity in the same vessel. Adherent leukocytes were determined as the number of leukocytes remaining stationary for at least 30 s/mm^2 of vessel wall surface.

Treatment and experimental groups for intravital microscopy. Three days after tumor cell implantation into the dorsal skinfold chamber preparation, animals were randomly assigned to four groups (n = 6 or 7, respectively). On days 3, 5, and 7 after tumor cell implantation, one group of animals was treated by continuous i.v. infusion of EndoTAG-1 over 90 min. These cationic liposomes (20 mmol/L total lipid; injection volume: 10 mL/kg body weight) contained 0.5 mg/mL paclitaxel yielding a dose of 5 mg paclitaxel per kilogram of body weight.

Animals of control groups received conventional paclitaxel in Cremophor EL (Taxol; 5 mg/kg body weight), cationic liposomes devoid of paclitaxel, or just the solvent 5% glucose using injection volumes identical to those of the EndoTAG-1 group. Therefore, Taxol was diluted in 5% glucose before infusion, giving a paclitaxel concentration of 0.5 mg/mL. Moreover, liposomes without paclitaxel in a lipid composition identical to EndoTAG-1 were used at the same lipid dose (20 mmol/L total lipid).

Using *in vivo* fluorescence microscopy, leukocyte-endothelial cell interactions were analyzed on day 7 and microvascular permeability was quantified on day 10 after tumor cell implantation. After sacrificing the animals by an overdose of pentobarbital on day 10, H&E-stained sections of the tumors were analyzed for leukocyte infiltration.

Analysis of the targeting properties of cationic liposomes after repeated EndoTAG-1 treatment. In separate experiments using untreated (n = 2) and EndoTAG-1–treated (n = 4) animals, rhodamine-labeled cationic liposomes (10 mmol/L, 10 μL/g body weight) were given i.v. over 90 min on day 10 after tumor cell implantation.

Visualization of the fluorescently labeled cationic liposomes was done using *in vivo* fluorescence microscopy 2, 4, and 6 h after administration. After 24 h, FITC-labeled lectin (1 mg/mL *Lycopersicon esculentum*, Vector) was injected (4 mg/kg body weight) as a vascular marker. FITC-lectin was allowed to circulate for 30 s before animals were sacrificed. Cryosections (20 μm) of tumor tissue were collected on polylysine-coated slides (Menzel), covered with Vectashield (Vector Laboratories), and subsequently examined using a Zeiss Axiophot 2 fluorescence microscope (Zeiss) with specific filter sets for FITC-, rhodamine-, and FITC/rhodamine double fluorescence and ×10 and ×40 objectives.

Subcutaneous tumor growth. The dorsal skin of hamsters (70 ± 5 g body weight) was shaven and chemically depilated under general anesthesia. A-Mel-3 tumor cells (4×10^6 to 6×10^6) were suspended in 10 μL RPMI 1640 (Biochrom) and injected s.c. into the lumbosacral region of the dorsal skin. The longer (l) and the shorter (w) perpendicular axes and the height (h) of each tumor nodule were measured by caliper, and tumor volume was calculated according to the following formula (20):

$$V_t = 0.837 \cdot l \cdot w \cdot h$$

Treatment and experimental groups for combination therapy of subcutaneous tumors. Twenty-four hours before treatment start, permanently indwelling fine polyethylene catheters (PE10) were implanted into the right jugular vein. On days 5, 7, and 9 after tumor cell implantation, the following four groups of animals were treated (n = 6 or 7 per group): EndoTAG-1 and cationic liposomes devoid of paclitaxel were given i.v. by a continuous infusion over 90 min. Further control groups received cisplatin alone (0.75 mg/kg body weight Platinex, Bristol-Myers Squibb) or NaCl (0.9%), both given in equivalent volumes by i.p. injection. When given in addition to EndoTAG-1, cisplatin was injected immediately after the 90-min infusion. Animals were sacrificed on day 11 after tumor cell inoculation by an overdose of pentobarbital (Nembutal, Sanofi-Leva). Cryosections (10 μm) of tumor tissue were examined using an Axioskop 40 microscope (Zeiss) with ×20 and ×100 objectives.

Statistical analysis. Results are presented as mean ± SE. Data were evaluated using the Friedman repeated measures ANOVA on ranks and Kruskal-Wallis ANOVA on ranks, respectively (SigmaStat; Jandel Scientific). P values smaller than 5% were considered to be significant.

Results

Microvascular leakiness after EndoTAG-1 treatment. Tumors were allowed to grow for 3 days and to induce angiogenesis verified by light microscopy before animals were assigned into four groups and treatment started. All animals tolerated the treatments well and there were no obvious signs of discomfort and no body weight loss.

Representative ROIs were chosen after administration of FITC-dextran, highlighting functional tumor microvessels. Compared with control groups, functional vessel density was obviously reduced after vascular targeting therapy using EndoTAG-1 (Fig. 1, *left*).

After the assessment of background fluorescence intensity (0 min) using a rhodamine-specific filter block, a bolus injection of rhodamine-labeled albumin was given i.v. In Fig. 1, representative images from the measurements in the different treatment groups are displayed. In control groups treated with glucose, paclitaxel alone, or cationic liposomes devoid of paclitaxel, there was a continuous slight increase of the fluorescence signal related to fluorescent albumin in the extravascular compartment after 2, 5, and 15 min, respectively. However, the increase of extravascular fluorescence intensity was stronger after treatment with EndoTAG-1 even with regard to the obviously rather low functional vessel density (Fig. 1, *left*).

For quantitative analysis of microvascular permeability for albumin, not only fluorescence intensity in every respective ROI but also the ratio of vascular volume and vascular surface was analyzed, thus reflecting different vessel densities (Table 1). Although the ratio of vascular volume and vascular surface was comparable between the groups, $(\mathrm{d}I/\mathrm{d}t) / (I_0\text{-}I_b)$ was significantly increased after treatment with CL and EndoTAG-1.

In comparison with glucose-treated tumors ($P_{\text{Glc}} = 1.3 \times 10^{-7} \pm 1.2 \times 10^{-8}$ cm/s), intratumoral microvascular permeability

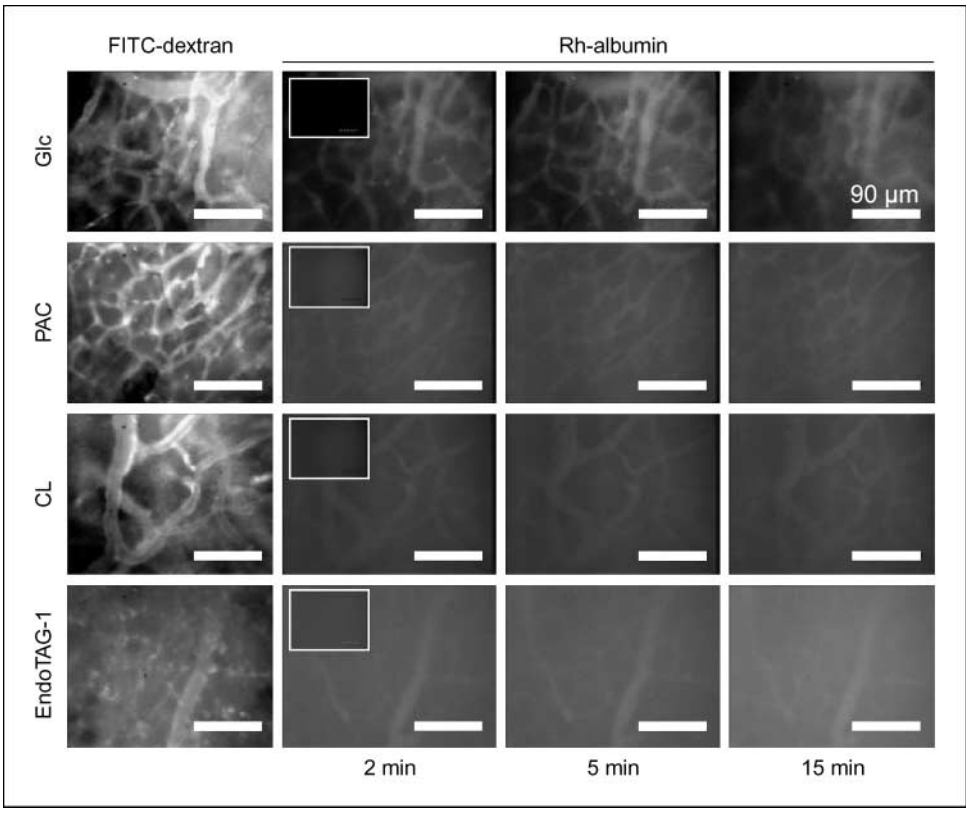

Fig. 1. *In vivo* fluorescence microscopy of microvascular leakiness after repeated EndoTAG-1 therapy: After the assessment of background fluorescence intensity at 0 min (see *insets in second column*) using a rhodamine-specific filter block, a bolus injection of rhodamine-labeled albumin was given i.v. In control groups treated with glucose (*Glc*), paclitaxel alone (*PAC*), or cationic liposomes devoid of paclitaxel (*CL*), respectively, there was a continuous slight increase of the fluorescence signal related to fluorescent albumin in the extravascular compartment after 2, 5, and 15 min. Nevertheless, the increase of extravascular fluorescence intensity was stronger after treatment with EndoTAG-1 even with regard to the obviously rather low functional vessel density (*left*).

for albumin was increased in all other groups; however, the changes observed among tumors treated with paclitaxel alone (P_{PAC} = 2.8 × 10^{-7} ± 6.9 × 10^{-8} cm/s) or cationic liposomes devoid of paclitaxel (P_{CL} = 2.7 × 10^{-7} ± 4.6 × 10^{-8} cm/s) were not significant (Fig. 2). Only after treatment with EndoTAG-1, microvascular permeability for albumin was significantly increased ($P_{EndoTAG-1}$ = 3.7 × 10^{-7} ± 3.9 × 10^{-8} cm/s) and >2-fold higher compared with glucose-treated controls.

Leukocyte-endothelial cell interactions after EndoTAG-1 treatment. Because inflammatory reactions are able to affect microvascular permeability, we quantified all qualities of leukocyte-endothelial cell interactions among the groups after three treatments. At comparable leukocyte flux values (Fig. 3A), the fraction of rolling leukocytes (Fig. 3B) and leukocyte adherence (Fig. 3C) revealed no significant changes in any group. Furthermore, permeability data and leukocyte adherence data were not correlated ($P > 0.05$; Spearman's correlation coefficient 0.28; data not shown). Hence, changes of intratumoral microvessel leakiness are unlikely to be caused by inflammatory reactions mediated by leukocytes.

Targeting properties of cationic liposomes after EndoTAG-1 treatment. To analyze the targeting properties of cationic liposomes after repeated therapy and to answer the question whether extravasation occurs due to the increase in microvascular leakiness, rhodamine-labeled cationic liposomes were infused 3 days after the last EndoTAG-1 treatment (day 10). *In vivo* fluorescence microscopy revealed that cationic liposomes were still targeting tumor microvasculature (Fig. 4). Peak fluorescence intensity was observed after 2 h—and thus 30 min after the end of the infusion (Fig. 4A)—and was also detectable after 4 h (Fig. 4B) and 6 h (Fig. 4C). In these experiments, the fluorescence signal in tumors treated with EndoTAG-1 revealed no significant difference compared with untreated control tumors. Subsequent double-fluorescence histology revealed colocalization of microvessels and cationic liposomes even after 24 hours (Fig. 4D). In spite of high microvascular permeability for albumin, there were no signs of extravasation of cationic liposomes up to this time point.

Tumor growth after combination therapy of EndoTAG-1 and cisplatin. The increase of microvascular leakiness after

Table 1. Results of measurements for permeability analysis

	Glc	PAC	CL	EndoTAG-1
(dI/dt) / (I_0-I_b), AU	5.5 × 10^{-5} ± 2.4 × 10^{-5}	3.6 × 10^{-4} ± 1.0 × 10^{-4}	4.6 × 10^{-4} ± 8.0 × 10^{-5}*	7.9 × 10^{-4} ± 2.2 × 10^{-4}*
V/S, cm	4.1 × 10^{-4} ± 2.4 × 10^{-5}	4.5 × 10^{-4} ± 7.0 × 10^{-5}	4.0 × 10^{-4} ± 4.8 × 10^{-5}	4.6 × 10^{-4} ± 6.0 × 10^{-5}
P, cm/s	1.3 × 10^{-7} ± 1.2 × 10^{-8}	2.8 × 10^{-7} ± 6.9 × 10^{-8}	2.7 × 10^{-7} ± 4.6 × 10^{-8}	3.7 × 10-7 ± 3.9 × 10^{-8}*

Abbreviations: Glc, glucose; PAC, paclitaxel; CL, cationic liposomes without paclitaxel.
*$P < 0.05$ versus glucose.

EndoTAG-1 therapy favored the evaluation of a combination therapy adding a small molecular substance directed against the tumor cells. Therefore, antitumoral efficacy of the combination therapy of EndoTAG-1 and cisplatin was analyzed in s.c. growing A-Mel-3 tumors. Animals tolerated the treatment well, gained weight, and did not show significant differences in body weight over the observation period of 11 days.

Already on day 7 after tumor cell inoculation, i.e., 2 days after first treatment, there was a delay in tumor growth after treatment with the combination therapy compared with the control groups treated with NaCl, cisplatin, and cationic liposomes devoid of paclitaxel, respectively (Fig. 5A). Only the combination therapy resulted in a significant reduction of tumor growth comparing with NaCl-treated animals, which was maintained until the end of the observation period.

Histologic analysis after combination therapy of EndoTAG-1 and cisplatin. Histologic analysis (H&E) of NaCl-treated s.c. A-Mel-3 tumors (Fig. 5B) revealed dense tumor cells with low tumor stroma content. In contrast, insular necrotic areas were detectable in EndoTAG-1–treated tumors possibly derived from occluded microvessels. In accordance with the rather low extent of leukocyte-endothelial cell interactions in A-Mel-3 tumors *in vivo*, leukocyte infiltration that might occur due to leukocyte migration into tumor stroma was also absent in tumors treated with EndoTAG-1 as well as in the other groups.

After cisplatin treatment, some loose necrotic tumor cells were observed but there were essentially no occluded vessels. Finally, after the combination therapy of anti-tumor cell–directed cisplatin and antivascular EndoTAG-1 occluded vessels were observed as well as clusters of necrotic tumor cells that were often found in the vicinity of the microthrombosis formation.

Discussion

Because cationic liposomes have been shown to selectively accumulate in activated tumor microvessels, cationic liposomes seem to be promising carriers directing chemotherapeutic substances to the tumor endothelium for the realization of a vascular targeting concept of therapy (7). In earlier studies, it was shown that encapsulation of paclitaxel in cationic liposomes (EndoTAG-1) significantly increases the antitumoral efficacy of the drug (8). Furthermore, quantitative *in vivo* as well as histologic findings of tumor-selective vessel occlusions by platelets (10) with a significant reduction of functional vessel density and a dramatic impairment of tumor perfusion along with increased tumor endothelial cell apoptosis (9) support vascular targeting as the underlying mechanism.

The data presented here show that vascular targeting with EndoTAG-1 significantly increases tumor microvessel leakiness without affecting the targeting properties of cationic liposomes. This seems to be due to direct vascular damage and is less likely to be mediated by inflammatory changes, e.g., leukocyte-endothelial cell interactions. Finally, vascular targeting with EndoTAG-1 enables effective combination therapy with small molecular cisplatin targeted at tumor cells.

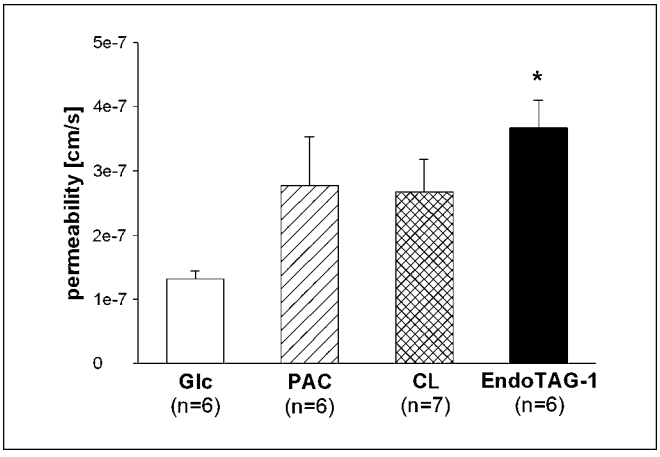

Fig. 2. Quantitative analysis of microvascular permeability for albumin after repeated EndoTAG-1 therapy: In comparison with glucose-treated tumors, intratumoral microvascular permeability for albumin was increased in all other groups, but the changes observed among tumors treated with paclitaxel alone or cationic liposomes devoid of paclitaxel were not significant. Only after treatment with EndoTAG-1, microvascular permeability for albumin was significantly increased and was >2-fold higher compared with glucose-treated controls. *, $P < 0.05$ versus glucose. *Columns,* mean; *bars,* SE.

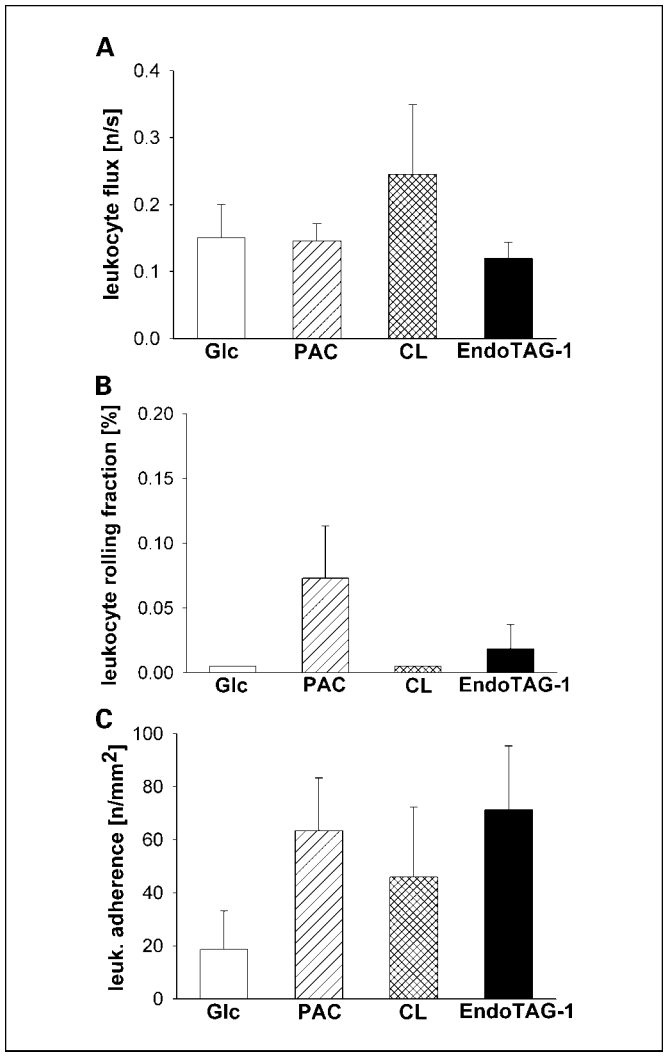

Fig. 3. Leukocyte-endothelial cell interactions after repeated EndoTAG-1 therapy: At comparable leukocyte flux values (*A*), the fraction of rolling leukocytes (*B*) and leukocyte adherence (*C*) revealed no significant changes in any group.

Thurston et al. (7) showed that cationic liposomes preferentially accumulate in angiogenic tumor endothelia after i.v. injection. Considering intratumoral microvascular damage induced by EndoTAG-1, the hypothesis that the blood-tumor barrier becomes more leaky needed to be experimentally addressed. Furthermore, the questions can be raised how this is mediated and what consequences follow especially for the targeting properties of cationic liposomes as well as for combination therapy regimen using EndoTAG-1.

For example, combretastatin A4, a drug with well-known vascular targeting property, increased microvascular permeability *in vivo* (13) and even susceptibility of tumors to treatment was shown to depend on microvascular permeability assessed by dynamic magnetic resonance imaging measurements (21). In this context, Tozer et al. postulated a contribution of leukocyte-endothelial cell interactions to the vascular shutdown seen after vascular targeting with combretastatin A4. In this scenario, leukocyte adhesion might increase the oxidative stress, followed by leukocyte infiltration leading to tumor cell death (13). It is well known that leukocyte-endothelial cell interactions can increase microvascular permeability (12). Nevertheless, expression of leukocyte adhesion molecules in tumor endothelium is low (22). According to the data presented here, no significant effects of EndoTAG-1 therapy neither on leukocyte flux nor on leukocyte rolling nor on leukocyte adherence in tumor microvessels were observed. Leukocyte migration into the tumor did not occur in a significant extent. Hence, it is unlikely that leukocytes decisively contribute to the therapeutic effects of EndoTAG-1 or cause the changes in tumor microvascular permeability. Consequently, inflammatory or immunologic phenomena seem not to be crucial for the increase in microvascular permeability after EndoTAG-1 treatment. Considering intratumoral microthrombosis formation triggered by EndoTAG-1 therapy (10) and subsequent severely impaired functional tumor microcirculation and endothelial cell apoptosis within tumors (9), endothelial cell damage is the most likely reason for the increased microvascular permeability.

In this context, the question might be raised whether "normalization" of tumor microvessels occurs during antivascular therapy (23). Antiangiogenesis was shown to decrease microvessel resistance by loss of tortuosity and irregularity in microvessel diameters. This might result in an increased blood flow. If this accounts to improved drug delivery even if microvessel leakiness is decreased to some extent during normalization is still a matter of debate. However, our experimental findings using EndoTAG-1 as a vascular targeting formulation support the opposite: After repeated EndoTAG-1 treatment, microvessels seem more "irregular" with significantly smaller diameters (9). Therefore, resistance is supposed to be increased and blood flow is indeed significantly decreased (9). Finally, in the present study, the blood-tumor barrier was found to be significantly more leaky for albumin.

Intriguingly, the increased permeability may even become counterproductive: The mechanism of preferential accumulation of cationic liposomes and of their selective internalization by angiogenic tumor endothelial cells is still under evaluation, although an altered glycocalix of tumor endothelium has been hypothesized as a possible underlying mechanism. Anyway, if the substructures of the microvessels are significantly damaged during EndoTAG-1 treatment, a loss of the therapeutic target may occur. Although cationic liposomes used in this study (diameter ~140-160 nm) are larger than albumin (~7 nm), the leakiness of tumor microvessels for macromolecules is essentially caused by large pores (~200 nm-2 μm; refs. 1, 24) and the discontinuity of the basement membrane (4).

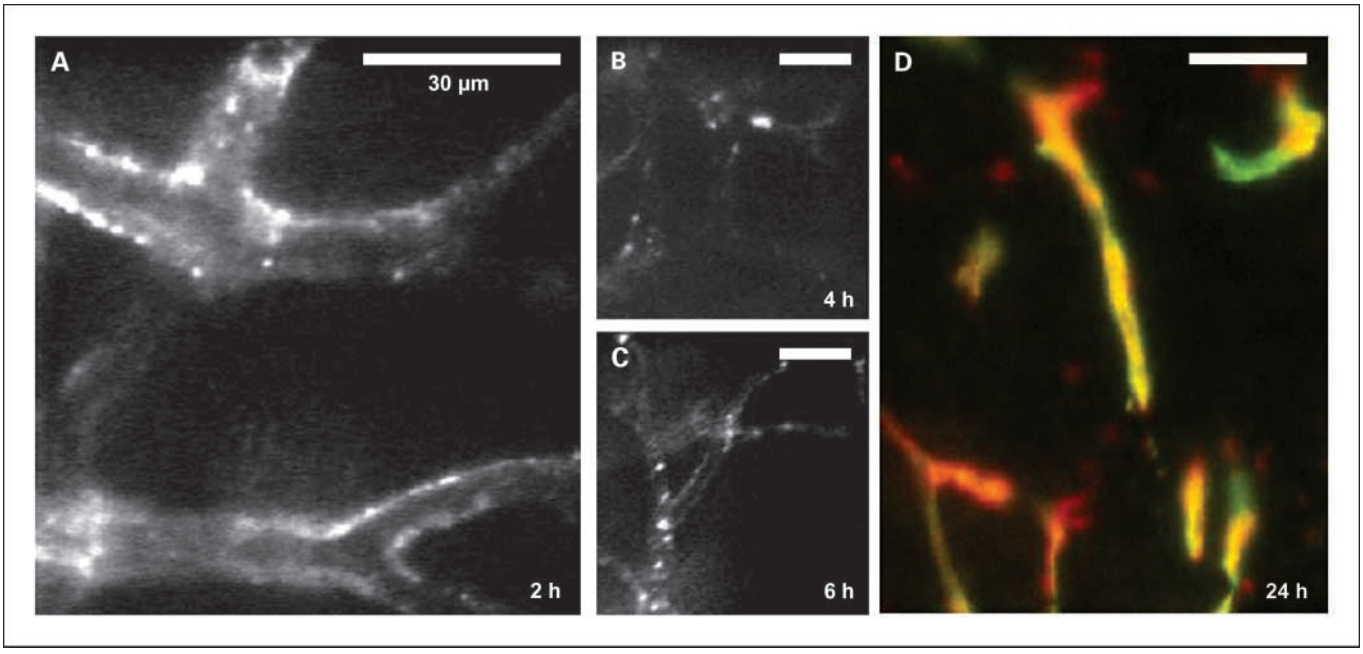

Fig. 4. Targeting properties of cationic liposomes after repeated EndoTAG-1 therapy: Peak fluorescence intensity was observed after 2 h (*A*), and thus 30 min after the end of the infusion, and was also detectable after 4 h (*B*) and 6 h (*C*). Subsequent double-fluorescence histology revealed colocalization (*yellow*) of microvessels (*green*) and cationic liposomes (*red*) even after 24 h (*D*). In spite of high microvascular permeability for albumin, there were no signs of extravasation of cationic liposomes up to this time point.

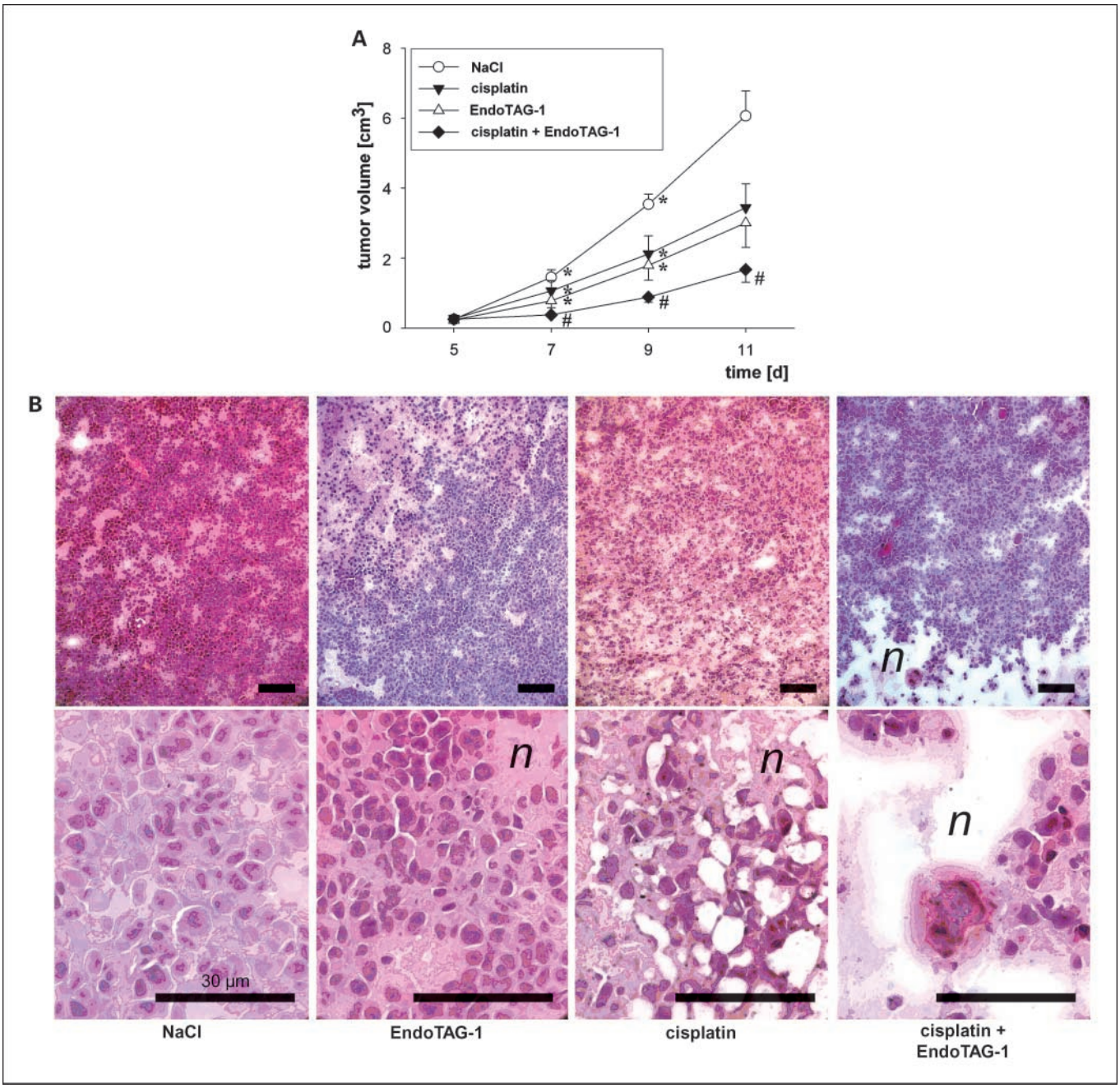

Fig. 5. Tumor growth and histologic analysis after combination therapy of EndoTAG-1 and cisplatin: Only the combination therapy resulted in a significant reduction of tumor growth (*A*) comparing with NaCl-treated animals that was maintained until the end of the observation period (*, $P < 0.05$ versus prior day of measurement; #, $P < 0.05$ versus NaCl). *Points,* mean; *bars,* SE. Histologic analysis (*B*) revealed insular necrotic spots after EndoTAG-1 monotherapy (*n,* necrosis). Loose necrotic tumor cells were observed after cisplatin monotherapy. However, only the combination therapy of cisplatin and EndoTAG-1 induced occluded tumor microvessels with clusters of necrotic tumor cells in the vicinity. Leukocyte infiltration was not detectable in all treated tumors.

Consequently, the extravasation of cationic liposomes used in this study was theoretically possible with respect to this pore cutoff size considering damaged tumor microvessels after repeated EndoTAG-1 treatment.

Nevertheless, it was clearly shown that the targeting properties of cationic liposomes were maintained even after repeated vascular targeting treatment using EndoTAG-1. As shown in an earlier study (14), localization of cationic liposomes after i.v. injection remained restricted to the vascular compartment in tumor tissue. After repeated treatment with EndoTAG-1, we found no signs of extravasation of fluorescently labeled cationic liposomes even 24 hours after injection. Hence, the target of this new antivascular approach is preserved even after repeated drug treatment, possibly due to a maintained net charge of the glycocalix. The preservation of the therapeutic target may even have implications against a possible development of resistance to EndoTAG-1 therapy.

On the other hand, transvascular transport has long been postulated as prerequisite for good antitumoral effects of a drug. In addition to molecular surface net charge of the respective substances, the substance size is crucial for its delivery across the blood-tumor barrier (24, 25). Deliberately modifying the blood-tumor barrier by increasing tumor vessel permeability for small molecular substances can be an important effect of vascular targeting therapy using EndoTAG-1. An increase of permeability for albumin (~7 nm) might in parallel reflect an enhanced diffusion of small molecular conventional chemotherapeutic substances into the tumor interstitium. Consequently, a therapeutic strategy combining a vascular targeting agent with a tumor cell–directed cytotoxic substance seemed a promising treatment strategy. Indeed, the combination therapy of EndoTAG-1 and cisplatin resulted in a significant tumor growth delay in A-Mel-3 tumors as well as in Lewis lung carcinomas (LLC-1; ref. 26). Although we did not show increased deposition of cisplatin itself within the tumor interstitium, the improved antitumor efficacy of the combination therapy using EndoTAG-1 and cisplatin might be an indirect proof of the hypothesis. In addition, histologic analysis revealed only after the combination of EndoTAG-1 and cisplatin necrotic tumor cell clusters preferentially in the vicinity of occluded microvessels that might be an indirect sign of increased microvessel leakiness by EndoTAG-1 and subsequent improved effectiveness of cisplatin among tumor cells. This is in line with immunohistochemical findings of vascular densities in treated LLC-1–bearing mice showing that cisplatin is contributing only little antivascular effects to the decrease in vessel density after combination with EndoTAG-1 (26).

It remains to be investigated whether microvascular permeability change is really linked to an initially decreased interstitial fluid pressure within the treated tumors (27) and whether the subsequent fluid influx with edema formation adds to the acute vascular shutdown reported for other vascular targeting agents (13). However, tumor growth effects and especially histologic data provide clear evidence for an additive effect of the combination of tumor vessel targeting EndoTAG-1 with tumor cell–directed conventional cisplatin chemotherapy. Considering combination therapies, timing and sequencing of antivascular agents and chemotherapeutic drugs need to be investigated in detail. In this study, cisplatin was administered directly after a 90-min infusion of EndoTAG-1. In contrast, other reports favor administration of vascular targeting agents after conventional chemotherapy (28). Thus far, the schedules to achieve most effective "trapping" or "delivery" of the cytotoxic drugs within the tumor by well-timed tumor-barrier modulation by vascular targeting still have to be defined systematically for the respective vascular targeting agent.

A mutual sensitization has been reported as the underlying mechanism for the combination of antivascular therapy and conventional chemotherapy (28, 29). In this context, apoptosis rates among endothelial cells were found to be significantly increased after the combination of ZD6126 and cisplatin (28). The increase of microvascular permeability appears as an additional novel mechanism for the successful combination of vascular targeting agents and conventional cytotoxic therapy.

Conclusions

Vascular targeting with EndoTAG-1 increases tumor microvessel leakiness significantly. This seems to be due to intratumoral vascular damage and is obviously not induced by inflammatory effects mediated by leukocytes. The targeting properties were maintained after repeated treatment with EndoTAG-1 as no signs of extravasation of cationic liposomes were observed. Deliberate manipulation at the blood-tumor barrier resulting in increased leakiness enables effective combination therapy of EndoTAG-1 and cisplatin, a small molecular substance of conventional chemotherapy.

Disclosure of Potential Conflicts of Interest

No potential conflicts of interest were disclosed.

Acknowledgments

We thank Christine Czapó and Alke Schropp at the Institute for Surgical Research, University of Munich, for technical assistance.

References

1. Hobbs SK, Monsky WL, Yuan F, et al. Regulation of transport pathways in tumor vessels: role of tumor type and microenvironment. Proc Natl Acad Sci U S A 1998;95:4607–12.
2. Morikawa S, Baluk P, Kaidoh T, et al. Abnormalities in pericytes on blood vessels and endothelial sprouts in tumors. Am J Pathol 2002;160:985–1000.
3. McDonald DM, Baluk P. Significance of blood vessel leakiness in cancer. Cancer Res 2002;62:5381–5.
4. Chang YS, di Tomaso E, McDonald DM, et al. Mosaic blood vessels in tumors: frequency of cancer cells in contact with flowing blood. Proc Natl Acad Sci U S A 2000;97:14608–13.
5. Denekamp J. The tumour microcirculation as a target in cancer therapy: a clearer perspective. Eur J Clin Invest 1999;29:733–6.
6. Thorpe PE. Vascular targeting agents as cancer therapeutics. Clin Cancer Res 2004;10:415–27.
7. Thurston G, McLean JW, Rizen M, et al. Cationic liposomes target angiogenic endothelial cells in tumors and chronic inflammation in mice. J Clin Invest 1998;101:1401–13.
8. Schmitt-Sody M, Strieth S, Krasnici S, et al. Neovascular targeting therapy: paclitaxel encapsulated in cationic liposomes improves antitumoral efficacy. Clin Cancer Res 2003;9:2335–41.
9. Strieth S, Eichhorn ME, Sauer B, et al. Neovascular targeting chemotherapy: encapsulation of paclitaxel in cationic liposomes impairs functional tumor microvasculature. Int J Cancer 2004;110:117–24.
10. Strieth S, Nussbaum CF, Eichhorn ME, et al. Tumor-selective vessel occlusions by platelets after vascular targeting chemotherapy using paclitaxel encapsulated in cationic liposomes. Int J Cancer 2008;122:452–60.
11. Eichhorn ME, Strieth S, Krasnici S, et al. Protamine enhances uptake of cationic liposomes in angiogenic microvessels. Angiogenesis 2004;7:133–41.
12. Michel CC, Curry FE. Microvascular permeability. Physiol Rev 1999;79:703–61.
13. Tozer GM, Prise VE, Wilson J, et al. Mechanisms associated with tumor vascular shut-down induced by combretastatin A-4 phosphate: intravital microscopy and measurement of vascular permeability. Cancer Res 2001;61:6413–22.
14. Krasnici S, Werner A, Eichhorn ME, et al. Effect of the surface charge of liposomes on their uptake by angiogenic tumor vessels. Int J Cancer 2003;105:561–7.
15. Asaishi K, Endrich B, Goetz A, Messmer K. Quantitative analysis of microvascular structure and function in the amelanotic melanoma A-Mel-3. Cancer Res 1981;41:1898–904.
16. Endrich B, Hammersen F, Goetz A, Messmer K. Microcirculatory blood flow, capillary morphology and local oxygen pressure of the hamster amelanotic melanoma A-Mel-3. J Natl Cancer Inst 1982;68:475–85.
17. Yuan F, Leunig M, Berk DA, Jain RK. Microvascular permeability of albumin, vascular surface area, and vascular volume measured in human adenocarcinoma LS174T using dorsal chamber in SCID mice. Microvasc Res 1993;45:269–89.
18. Klyscz T, Jünger M, Jung F, Zeintl H. Cap image-a

new kind of computer-assisted video image analysis system for dynamic capillary microscopy. Biomed Tech (Berl) 1997;42:168–75.

19. Zeintl H, Sack FU, Intaglietta M, Messmer K. Computer assisted leukocyte adhesion measurement in intravital microscopy. Int J Microcirc Clin Exp 1989;8:293–302.

20. Weiss N, Delius M, Gambihler S, et al. Influence of the shock wave application mode on the growth of A-Mel 3 and SSK2 tumors *in vivo*. Ultrasound Med Biol 1990;16:595–605.

21. Beauregard DA, Hill SA, Chaplin DJ, Brindle KM. The susceptibility of tumors to the antivascular drug combretastatin A4 phosphate correlates with vascular permeability. Cancer Res 2001;61:6811–5.

22. Langley RR, Russell J, Eppihimer MJ, et al. Quantification of murine endothelial cell adhesion molecules in solid tumors. Am J Physiol 1999;277:H1156–66.

23. Jain RK. Normalizing tumor vasculature with anti-angiogenic therapy: a new paradigm for combination therapy. Nat Med 2001;7:987–9.

24. Yuan F, Dellian M, Fukumura D, et al. Vascular permeability in a human tumor xenograft: molecular size dependence and cutoff size. Cancer Res 1995;55:3752–6.

25. Dellian M, Yuan F, Trubetskoy VS, Torchilin VP, Jain RK. Vascular permeability in a human tumour xenograft: molecular charge dependence. Br J Cancer 2000;82:1513–8.

26. Luedemann S, Eichhorn ME, Strieth S, et al. Antivascular tumor therapy by paclitaxel encapsulated in cationic lipid complexes (EndoTAG-1): comparison of metronomic and maximum tolerated dose treatment. Angiogenesis 2006;9:29.

27. Rubin K, Sjoquist M, Gustafsson AM, et al. Lowering of tumoral interstitial fluid pressure by prostaglandin E(1) is paralleled by an increased uptake of ([51])Cr-EDTA. Int J Cancer 2000;86:636–43.

28. Goto H, Yano S, Matsumori Y, et al. Sensitization of tumor-associated endothelial cell apoptosis by the novel vascular-targeting agent ZD6126 in combination with cisplatin. Clin Cancer Res 2004;10:7671–6.

29. Kerbel RS. Antiangiogenic therapy: a universal chemosensitization strategy for cancer? Science 2006;312:1171–5.